

The Kinetics and Mechanism of the Reaction of 5-Fluorocytosine with Hydroxylamine

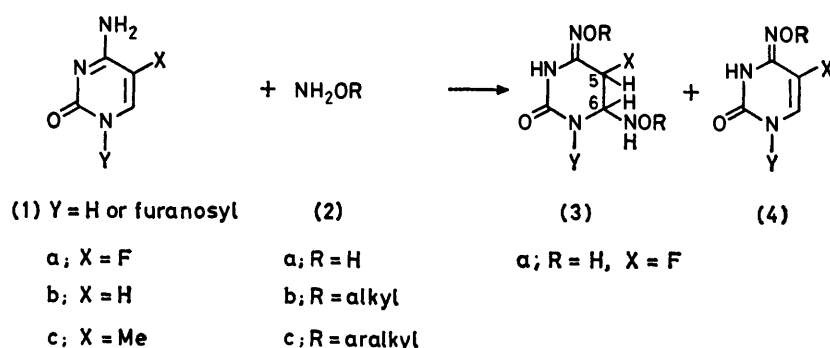
By David J. Palling, Paul J. Atkins, and C. Dennis Hall,* Department of Chemistry, King's College, University of London, Strand, London WC2R 2LS

Kinetic and stereochemical data on the reaction of 5-fluorocytosine (1a) with hydroxylamine (2a) to form 5-fluoro-3,4,5,6-tetrahydro-6-hydroxyamino-4-hydroxyiminopyrimidin-2(1*H*)-one (3a) are presented. A mechanistic scheme involving acid catalysis and a change in the rate-limiting step with increasing hydroxylamine concentration is proposed.

INTEREST in the reaction of cytosines with hydroxylamines began with the discovery by Freese *et al.*¹⁻⁴ that hydroxylamines are able to cause mutations in some T-even bacteriophages at or near neutral pH. This effect

EXPERIMENTAL

Kinetic Measurements.—The rates of reaction were followed by monitoring the disappearance of (1a) at 280 nm using 10 mm cuvettes thermostatted at 38 °C in the cell



is accepted as being due to interaction with cytosine residues. Further synthetic, mechanistic, and stereochemical studies have been carried out by Budowsky,⁵⁻⁹ Lawley,¹⁰ Brown,¹¹⁻¹⁶ and more recently, by Blackburn¹⁷⁻¹⁹ and Hall.^{20,21}

housing of a Unicam SP 1700 spectrophotometer. The ionic strength was maintained at 4.0M by the addition of NaCl and the pH was maintained by the buffering action of hydroxylamine hydrochloride partially neutralised by sodium hydroxide. The reactions were carried out under

TABLE I

Values of k_{obs} , for the reaction of 5-fluorocytosine with hydroxylamine at 38 °C

pH	5.24 (22.4) ^a	5.47 (32.9)	5.60 (39.8)	5.87 (55.2)	6.06 (65.6)	6.43 (81.7)	6.98 (94.1)
$[\text{NH}_2\text{OH}]/\text{M}$	$10^5 k_{\text{obs}}/\text{s}^{-1}$	$10^5 k_{\text{obs}}/\text{s}^{-1}$	$10^5 k_{\text{obs}}/\text{s}^{-1}$	$10^5 k_{\text{obs}}/\text{s}^{-1}$	$10^5 k_{\text{obs}}/\text{s}^{-1}$	$10^5 k_{\text{obs}}/\text{s}^{-1}$	$10^5 k_{\text{obs}}/\text{s}^{-1}$
0.5	2.35	3.65	3.05	3.57	3.08	2.41	1.09
1.0	7.12	9.31	9.83	10.2	9.14	7.61	3.19
1.5	13.3	16.6	17.3	19.7	17.3	13.6	6.31
2.0	19.0	24.1	26.1	28.1	25.6	20.4	9.30
2.5	29.8	33.5	35.0	35.8	35.3	27.9	12.4
3.0	37.1	46.2	42.6	43.4	42.8	34.0	15.1
3.5	43.2	51.8	49.6	55.8	45.6	41.0	18.7
4.0	48.1	54.3	56.7	60.7	52.2	47.2	21.7

^a Figures in parentheses represent % free hydroxylamine.

In general the reaction yields a mixture of a tetrahydropyrimidinone (3) and a 4-hydroxyiminouracil (4) and both types of product have been thoroughly characterised.²⁰ In the past kinetic measurements were carried out using cytosine, 1-methylcytosine, and 1,3-dimethylcytosine as substrates and the analysis was complicated by the formation of both products (3) and (4).⁵⁻¹⁹ The present study was performed using 5-fluorocytosine (1a; Y = H) since in this case the kinetic analysis was simplified by the formation of only one product (3a).

pseudo-first-order conditions with the initial concentration of (1a) at *ca.* 10^{-4}M and the total hydroxylamine concentration ranging from 0.5 to 4.0M. Rate constants were calculated by the Guggenheim method²² over at least three half-lives. Calculations were carried out with the aid of appropriate programs on the University of London CDC 6000 computer.

Several series of kinetic runs were made at fixed pH values and the proportion of hydroxylamine in the free base form, $[\text{NH}_2\text{OH}]_{\text{F}}$, was calculated using the Henderson-Hasselbach equation.²³ The $\text{p}K_{\text{a}}$ of hydroxylamine was

determined by automatic titration (Radiometer) and was found to be 5.78 ± 0.01 . All kinetic measurements were carried out at least in duplicate using doubly-distilled (from glass) deionised water.

RESULTS AND DISCUSSION

Kinetics.—The observed pseudo-first-order rate constants, k_{obs} (Table 1) show a bell-shaped curve when plotted against pH with a maximum at *ca.* pH 5.8 (Figure 1) and, contrary to our earlier report,²¹ a greater than first-order dependence on the total hydroxylamine concentration, $[\text{NH}_2\text{OH}]_{\text{T}}$, at a given pH (Figure 2). These results suggest that the hydroxylammonium ion acts as a catalyst. The upward curvature of the lines in Figure 2 reflects the component of the reaction which is second order in hydroxylamine. Inspection suggests that this curvature and hence the second-order component, becomes less significant as $[\text{NH}_2\text{OH}]_{\text{T}}$ is increased and this is confirmed by plots of the apparent second-order rate constants ($k_{2, \text{app}} = k_{\text{obs}}/[\text{NH}_2\text{OH}]_{\text{F}}$) against $[\text{NH}_2\text{OH}]_{\text{T}}$ (Figure 3). The initial slopes of the lines in Figure 3 are the rate constants for the catalysed reaction and since the values of $k_{2, \text{app}}$ are larger in the more acidic solutions it can be concluded that the hydroxylammonium ion is a more effective catalyst than free hydroxylamine. The lines extrapolate to zero

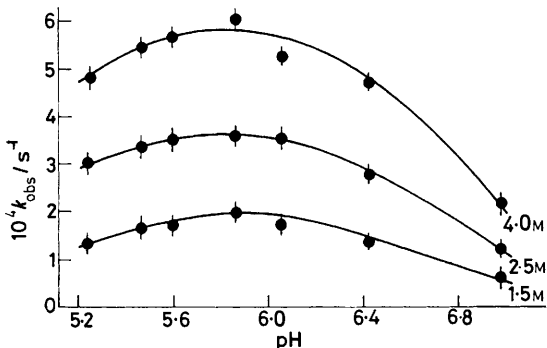


FIGURE 1 pH-Rate profiles for the reaction of 5-fluorocytosine with hydroxylamine at 38 °C

indicating that the uncatalysed reaction of hydroxylamine makes no detectable contribution to the observed rates.

The slopes of the lines in Figure 3 are large at low hydroxylamine concentration and tend to zero at higher hydroxylamine concentrations where the reaction becomes essentially independent of the catalyst concentration. This 'decrease' in the catalytic constant is evidence for a change in the rate-limiting step of the reaction with increasing hydroxylamine concentration. Thus, hydroxylammonium ion catalysis is important for the step which is rate limiting at low $[\text{NH}_2\text{OH}]_{\text{T}}$ but is negligible for the step which becomes rate limiting at high $[\text{NH}_2\text{OH}]_{\text{T}}$.

The reaction mixtures were also scanned periodically between 210 and 320 nm. A typical result is shown in Figure 4. At free hydroxylamine concentrations below *ca.* 1.4M an isosbestic point could be seen at 235 nm.

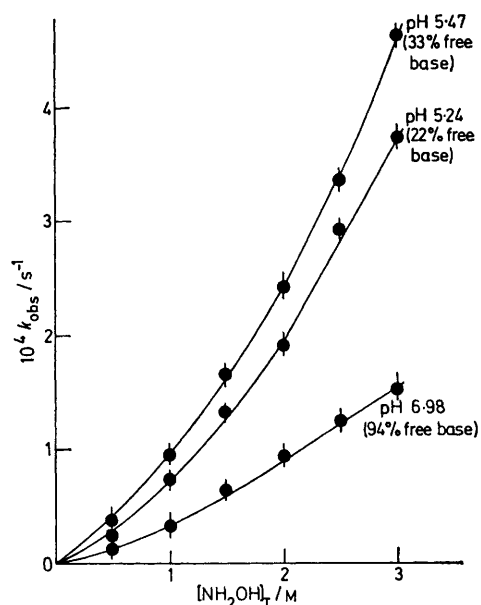


FIGURE 2 Plots of k_{obs} versus $[\text{hydroxylamine}]_{\text{T}}$ for the reaction of 5-fluorocytosine with hydroxylamine at 38 °C

Above this concentration the hydroxylamine blanks out the spectrum below 235 nm. An isosbestic point indicates that an intermediate is not accumulating during the reaction²⁴ and hence, at these lower concentrations certainly, the rate-limiting step is seen as the formation of the addition intermediate (5).

Stereochemistry.—The ¹⁹F and ¹H n.m.r. studies (Table 2) show that addition of hydroxylamines across the 5,6-double bond is highly stereoselective and *trans*.²¹ The signal : noise ratio (and hence the certainty of no *cis*-product in the sample) was better than 99% and only one product was detected in the reaction mixture by t.l.c.

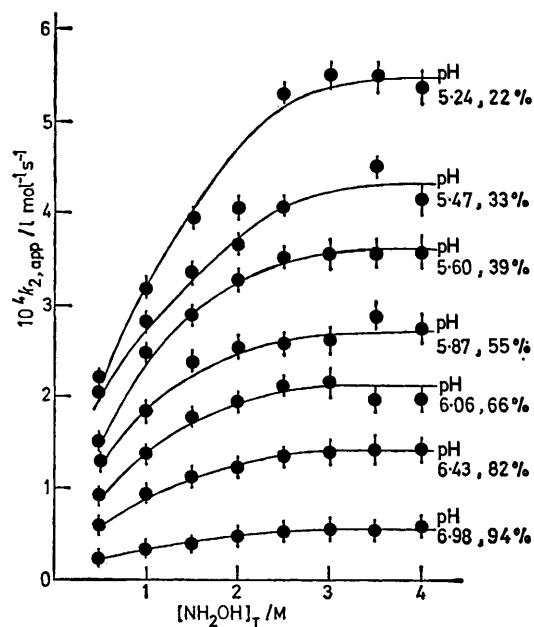


FIGURE 3 Plots of $k_{2, \text{app}}$ versus $[\text{NH}_2\text{OH}]_{\text{T}}$ for the reaction of 5-fluorocytosine with hydroxylamine

Incidentally, the value of $J_{\text{F}, 6-\text{H}}$ (18–20 Hz) denotes an *anti*-disposition of F-5 and 6-H^{25,26} and this is only compatible with the β -conformer of *trans*-addition. No changes in the ¹H n.m.r. spectra were observed on raising

For convenience this equilibrium has been summarised under K_1 . In principle, attack by free hydroxylamine on protonated (1a) may occur at C-4 or -6 but since these mechanisms are kinetically indistinguishable, extra-

TABLE 2

¹H and ¹⁹F n.m.r. of the pyrimidone (3a; X = F)

R	5-H		6-H		6-NH
	J_{gem}/Hz	$J_{4-\text{H}}/\text{Hz}$	$J_{5-\text{F}}/\text{Hz}$	J_{NH}/Hz	$J_{5-\text{F}}/\text{Hz}$
H	49.0	1.0	21.0	9.0	
Bu [†]	49.0	2.5	18.0	12.0	1.5
PhCH ₃	49.0	1.0	20.0	10.0	2.0

cis-addition *trans*-addition

the temperature to 60 °C and one must conclude that the energy barrier to interconversion of the α - and β -conformers is at least 20 kcal mol⁻¹.

Proposed Mechanism.—On the basis of the kinetic and stereochemical data there is a change in the rate-limiting step as $[\text{NH}_2\text{OH}]_T$ increases and the three further points which require an explanation are as follows. (1) Hydroxylammonium ion catalysis is more important for the reaction step which is rate limiting at low $[\text{NH}_2\text{OH}]_T$. (2) At low $[\text{NH}_2\text{OH}]_T$ there is no discernible build-up of an intermediate. (3) Addition across the 5,6-double bond is stereoselective and *trans*. A mechanism which would account for the data is shown in Scheme 1.

The first step may be regarded as a composite of three steps involving protonation of (1a) at N-3 by NH_3OH^+ ,

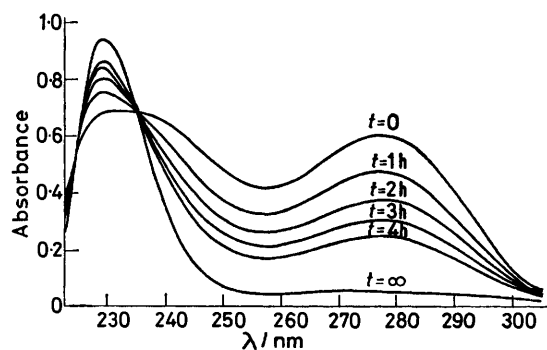
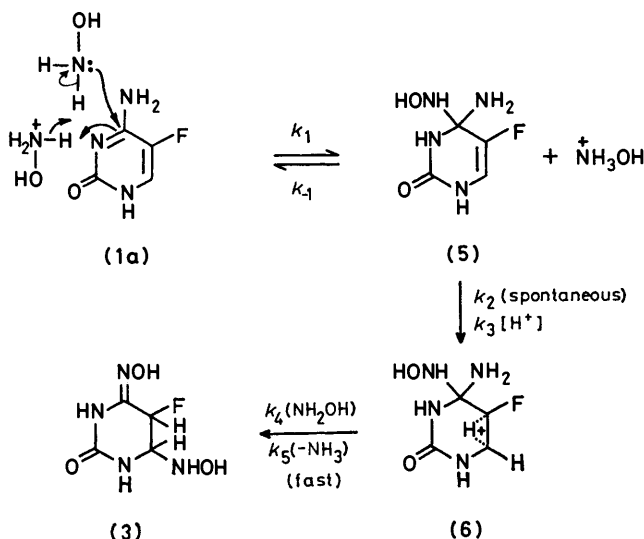


FIGURE 4 Absorbance curves for the reactions of 5-fluorocytosine with hydroxylamine at 38 °C, pH 5.5 (35% free base), and 1.0M-NH₂OH

attack by free hydroxylamine on the protonated substrate, and removal of a proton from the intermediate by excess free base, the proton-transfer steps being fast.

kinetic arguments are necessary to resolve the problem. In the past C-6 has been the preferred site¹⁹ but ¹³C n.m.r. spectra reveal that C-4 is the more electrophilic



SCHEME 1

carbon atom^{20,21} and the stereoselective *trans*-addition is more easily rationalised by initial attack at C-4.

At low $[\text{NH}_2\text{OH}]_T$, the formation of (5) is seen as rate limiting and is catalysed by NH_3OH^+ . At higher concentrations of (2) as the rate of formation of (5) increases, the proton transfer step (5) \rightarrow (6) becomes rate limiting. This step is analogous to the predominantly specific acid-catalysed hydration of olefins.^{27,28} Although it is recognised that general acid-catalysis

* As shown in the kinetic analysis section, catalysis of this step by the proton is not detectable.

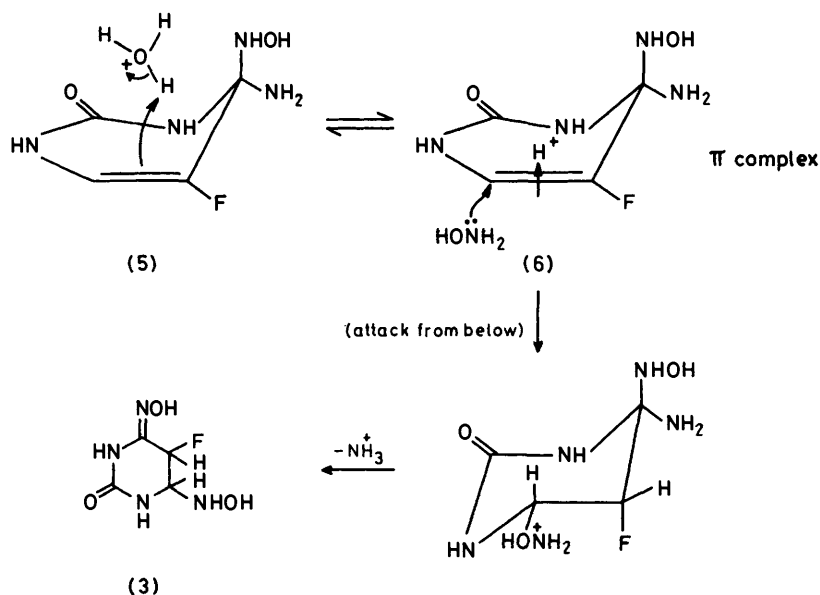
TABLE 3

Values of k_1 from plots of $[\text{NH}_2\text{OH}]_F/k_{\text{obs}}$ versus $1/[\text{NH}_3\text{OH}]^+$ at various pH values

pH	5.24	5.47	5.60	5.87	6.06	6.43	6.98
$10^4 k_1 / \text{l}^2 \text{mol}^{-1} \text{s}^{-1}$	7.4 ± 0.3	11.2 ± 1.0	7.7 ± 0.3	9.2 ± 0.4	8.4 ± 0.6	9.4 ± 0.2	11.1 ± 0.3

Average $k_1 = 9.2 \pm 1.5 \times 10^{-4} \text{l}^2 \text{mol}^{-1} \text{s}^{-1}$.

occurs in the hydration of vinyl ethers²⁹ and vinylamides,³⁰ the latter being a system which is analogous to (5),* it was not detectable in the 5-fluorocytosine system as evidenced by the levelling of $k_{2\text{att}}$ values with increasing $[\text{NH}_2\text{OH}]$ [cf. (3), (7), and (8)]. A plausible pathway for the reaction is shown in Scheme 2.

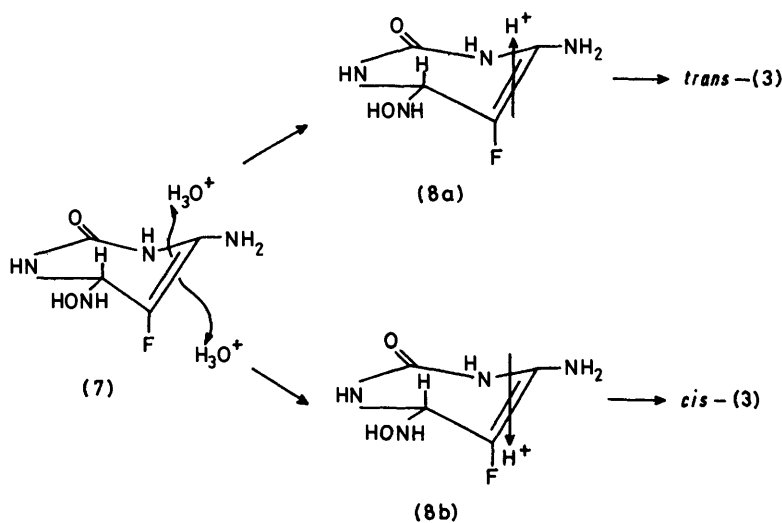


SCHEME 2

This mechanism parallels that proposed for the addition of hydrogen iodide to tiglic and angelic acids³¹ which is found to be stereoselective, *trans*. If one imagines initial addition of hydroxylamine to protonated

* We are indebted to a referee for alerting us to this work.

the reaction of hydroxylamine with amides,³² the propionic acid-catalysed formation of semicarbazone from acetophenone,³³ the borate-catalysed cyclisation of glutamine,³⁴ and the base-catalysed aminolysis of penicillin derivatives.³⁵



SCHEME 3

Kinetic Analysis.—The following analysis employs the steady-state approximation with respect to (5), *i.e.* $d[(5)]/dt = 0$ and thus its applicability to rates obtained at high $[\text{NH}_2\text{OH}]_{\text{F}}$ is possibly dubious.* Good agreement is obtained, however, between theory and the observed rates except at the very highest pH value investigated (pH 6.98; 94% free base).

$$d[(5)]/dt = k_1[\dot{\text{N}}\text{H}_3\text{OH}][\text{FC}][\text{NH}_2\text{OH}]_{\text{F}} - k_{-1}[\dot{\text{N}}\text{H}_3\text{OH}][(5)] - k_2[(5)] - k_3[(5)][\text{H}^+] \quad (1)$$

$$[(5)] = \frac{k_1[\dot{\text{N}}\text{H}_3\text{OH}][\text{NH}_2\text{OH}]_{\text{F}}[\text{FC}]}{k_{-1}[\dot{\text{N}}\text{H}_3\text{OH}] + k_2 + k_3[\text{H}^+]} \quad (2)$$

$$k_{\text{obs.}} = \frac{k_1[\dot{\text{N}}\text{H}_3\text{OH}][\text{NH}_2\text{OH}]_{\text{F}}(k_2 + k_3[\text{H}^+])}{k_{-1}[\dot{\text{N}}\text{H}_3\text{OH}] + k_2 + k_3[\text{H}^+]} \quad (3)$$

If FC = substrate, *i.e.* 5-fluorocytosine, equations (1) and (2) are obtained. Since, rate = $d[(3)]/dt = (k_2 + k_3[\text{H}^+])[(5)]$, $k_{\text{obs.}}$ is given by equation (3). Hence, equation (4) applies. Thus a plot of $[\text{NH}_2\text{OH}]_{\text{F}}/k_{\text{obs.}}$ versus $1/[\dot{\text{N}}\text{H}_3\text{OH}]$ at constant $[\text{H}^+]$ will give $1/k_1$ as

$$\begin{aligned} [\text{NH}_2\text{OH}]_{\text{F}}/k_{\text{obs.}} &= 1/k_{2, \text{app.}} = k_{-1}[\dot{\text{N}}\text{H}_3\text{OH}] + k_2 + k_3[\text{H}^+]/k_1[\dot{\text{N}}\text{H}_3\text{OH}](k_2 + k_3[\text{H}^+]) \\ &= k_{-1}/k_1(k_2 + k_3[\text{H}^+]) + 1/k_1[\dot{\text{N}}\text{H}_3\text{OH}] \end{aligned} \quad (4)$$

gradient and $k_{-1}/k_1(k_2 + k_3[\text{H}^+])$ as intercept (*e.g.* Figure 5). The gradients are independent of pH as required (Table 3).† From the intercept $I = k_{-1}/k_1(k_2 + k_3[\text{H}^+])$ one can obtain equation (5). Thus a

$$k_2/k_3 + [\text{H}^+] = k_{-1}/Ik_1k_3 \quad (5)$$

plot of $[\text{H}^+]$ against $1/I$ (Figure 6) will give an intercept of $-k_2/k_3$ and a gradient of k_{-1}/k_1k_3 . These and other ratios are shown in Table 4.

Using the values of Table 4, the plots shown in Figures 7 and 8 were obtained in which the $k_{2, \text{app.}}$ values are shown with error bars. The solid curves are calculated using the rate constant ratios and extrapolated back to the origin (dotted lines). The dashed lines in Figure 7

$$\begin{aligned} k_{\text{obs.}}/[\text{NH}_2\text{OH}]_{\text{F}} &= k_{2, \text{app.}} = k_1[\dot{\text{N}}\text{H}_3\text{OH}](k_2 + k_3[\text{H}^+])/k_{-1}[\dot{\text{N}}\text{H}_3\text{OH}] \\ &= K_1k_2 + K_1k_3[\text{H}^+] \end{aligned} \quad (6)$$

were calculated by making two approximations. At high concentrations of hydroxylamine when the proton transfer step (5) \rightarrow (6) becomes rate-limiting, $k_{-1}[\dot{\text{N}}\text{H}_3\text{OH}] \gg (k_2 + k_3[\text{H}^+])$. Hence, equation (6) is obtained. The horizontal, dashed lines represent the value of $k_{2, \text{app.}}$ and as expected, a plot of $k_{2, \text{app.}}$ (maximum) versus $[\text{H}^+]$ gives a straight line with a ratio of intercept/gradient = $k_2/k_3 = 1.88 \times 10^{-6}$ (*cf.* Table 4). At low $[\text{NH}_2\text{OH}]$ however, when the formation of (5) is rate limiting, we can assume $(k_2 + k_3[\text{H}^+]) \gg k_{-1}[\dot{\text{N}}\text{H}_3\text{OH}]$ and hence $k_{2, \text{app.}} = k_1[\dot{\text{N}}\text{H}_3\text{OH}]$. This situation is represented by the dashed lines at low $[\text{NH}_2\text{OH}]$.

* Because one cannot be certain that an isosbestic point occurs at high hydroxylamine concentrations.

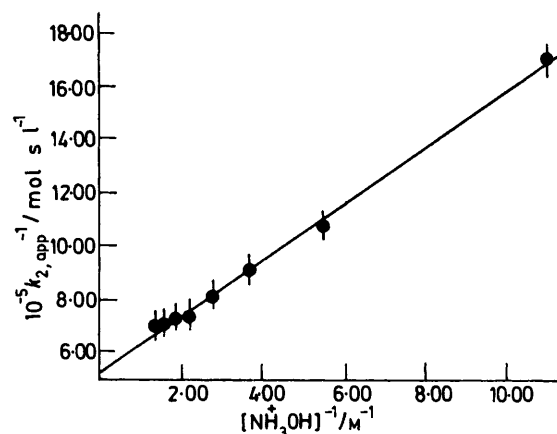


FIGURE 5 $1/k_{2, \text{app.}}$ versus $1/[\dot{\text{N}}\text{H}_3\text{OH}]$ for the reaction of 5-fluorocytosine with hydroxylamine at 38 °C and pH 6.43 (82% free base)

A calculated pH-rate profile compared with the experimental points is shown in Figure 9.

As indicated earlier the overall kinetic and mechanistic picture bears a very close similarity to that for the

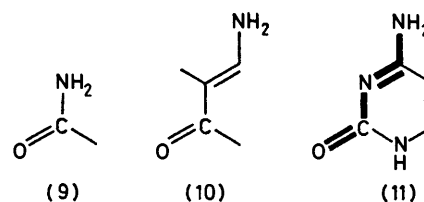
reaction of hydroxylamine with amides.³² The pH-rate profile is due to general acid catalysis whilst the change in rate-determining step occurs with increasing catalyst

TABLE 4

Rate coefficients ratios derived for the reaction of (1a) and (2a) in water at 38.0°

$10^4 k_1/I^2 \text{ mol}^{-2} \text{ s}^{-1}$	$= 9.18 \pm 1.37$
$10^3 k_{-1}/k_1 k_3 / \text{mol}^2 \text{ s}^{-1}$	$= 9.95 \pm 0.8$
$10^6 k_2/k_3 / \text{mol}^{-1}$	$= 1.86 \pm 0.33$
$10^6 k_{-1}/k_3$	$= 9.13$
$10^{-3} k_{-1}/k_1 k_2 / \text{mol} \text{ s}^{-1}$	$= 5.3$

concentration. In retrospect this is hardly surprising since cytosines may be regarded as cyclic vinylogues of amides [*cf.* (9), (10), and the section of (11) in bold] and



† If the formation of (5) was also catalysed to a significant extent by H_3O^+ , plots of $[\text{NH}_2\text{OH}]_{\text{F}}/k_{\text{obs.}}$ versus $1/[\dot{\text{N}}\text{H}_3\text{OH}]$ would not give straight lines.

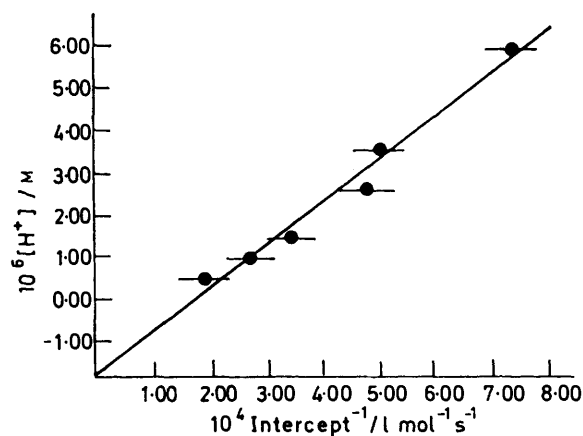


FIGURE 6 $1/\text{Intercept}$ (Figure 5) versus $[\text{H}^+]$ for the reaction of 5-fluorocytosine with hydroxylamine at 38 °C at various pH values

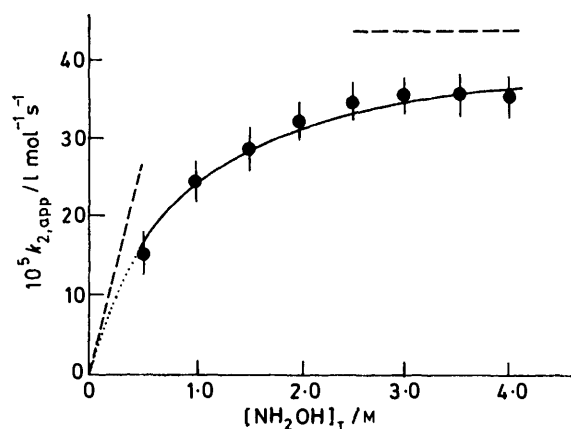


FIGURE 7 $k_{2,\text{app}}$ versus $[\text{NH}_2\text{OH}]_T$ at pH 5.60 (39.8% free base). The solid line is calculated from the rate coefficient shown in Table 4 and equation (3) (for explanation of dashed lines see text)

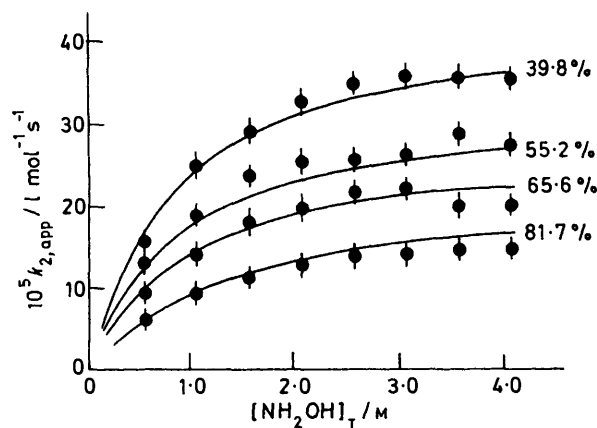


FIGURE 8 $k_{2,\text{app}}$ versus $[\text{NH}_2\text{OH}]_T$ at pH 5.60 (39.8% free base), 5.87 (55.2% free base), 6.06 (65.6% free base), and 6.43 (81.7% free base). The solid lines are calculated from the rate coefficients shown in Table 4 and equation (3)

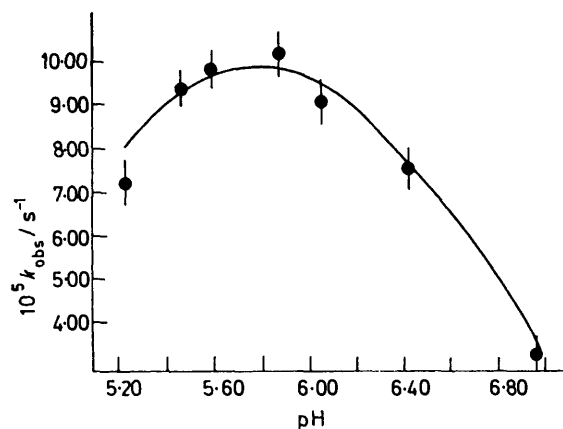


FIGURE 9 k_{obs} versus pH at 1.0M- $[\text{NH}_2\text{OH}]_T$. The solid line is calculated from the rate coefficient shown in Table 4 and a suitably rearranged version of equation (3)

We thank the Cancer Research Campaign for financial support.

[9/1856 Received, 22nd November, 1979]

REFERENCES

- 1 E. Freese, E. Bautz-Freese, and E. Bautz, *J. Mol. Biol.*, 1961, **3**, 133.
- 2 E. Freese, E. Bautz, and E. Bautz-Freese, *Proc. Nat. Acad. Sci. U.S.A.*, 1961, **47**, 845.
- 3 E. Freese and H. B. Strack, *Proc. Nat. Acad. Sci. U.S.A.*, 1962, **48**, 1796.
- 4 E. Bautz-Freese and E. Freese, *Proc. Nat. Acad. Sci. U.S.A.*, 1964, **52**, 1289.
- 5 N. K. Kochetkov, E. I. Budowsky, and R. P. Shibaeva, *Biochim. Biophys. Acta*, 1963, **68**, 493.
- 6 N. K. Kochetkov, E. I. Budowsky, E. D. Sverdlov, R. P. Shibaeva, V. N. Shibaev, and G. S. Monastirskaya, *Tetrahedron Letters*, 1963, 3253.
- 7 E. I. Budowsky, R. P. Shibaeva, E. D. Sverdlov, and G. S. Monastirskaya, *Molekulyarnaya Biologiya (English translation)*, 1968, **2**, 260.
- 8 E. I. Budowsky, E. D. Sverdlov, R. P. Shibaeva, G. S. Monastirskaya, and N. K. Kochetkov, *Molekulyarnaya Biologiya (English translation)*, 1968, **2**, 267.
- 9 E. I. Budowsky, E. D. Sverdlov, R. P. Shibaeva, G. S. Monastirskaya, and N. K. Kochetkov, *Biochim. Biophys. Acta*, 1971, **246**, 300.
- 10 P. D. Lawley, *J. Mol. Biol.*, 1967, **24**, 75.
- 11 D. M. Brown and J. H. Phillips, *J. Mol. Biol.*, 1965, **11**, 663.
- 12 D. M. Brown and P. Schell, *J. Chem. Soc.*, 1965, 208.
- 13 D. M. Brown and M. J. E. Hewlins, *J. Chem. Soc. (C)*, 1968, 1922.
- 14 D. M. Brown, M. J. E. Hewlins, and P. Schell, *J. Chem. Soc. (C)*, 1968, 1925.
- 15 D. M. Brown and M. J. E. Hewlins, *J. Chem. Soc. (C)*, 1968, 2050.
- 16 D. M. Brown and P. F. Coe, *Chem. Comm.*, 1970, 568.
- 17 G. M. Blackburn, S. Jarvis, M. C. Ryder, and V. Solan, *J.C.S. Perkin I*, 1975, 370.
- 18 G. M. Blackburn, V. Solan, D. M. Brown, and P. F. Coe, *J.C.S. Chem. Comm.*, 1976, 724.
- 19 G. M. Blackburn and V. Solan, *J.C.S. Perkin II*, 1977, 609.
- 20 P. M. Schalke and C. D. Hall, *J.C.S. Perkin I*, 1975, 2416.
- 21 P. M. Schalke and C. D. Hall, *J.C.S. Chem. Comm.*, 1976, 391.
- 22 E. A. Guggenheim, *Phil. Mag.*, 1926, **2**, 538.
- 23 W. P. Jencks, 'Catalysis in Chemistry and Enzymology,' McGraw-Hill, New York, 1969.
- 24 J. F. Bunnett in 'Techniques of Chemistry. Vol. VI, part 1. Investigation of Rates and Mechanisms of Reactions,' ed. E. S. Lewis, Wiley-Interscience, New York, 1974, 3rd edn. p. 176.
- 25 A. Peake and L. F. Thomas, *Trans. Faraday Soc.*, 1966, **62**, 2980.

- ²⁶ L. D. Hall and D. L. Jones, *Canad. J. Chem.*, 1973, **51**, 2925.
²⁷ V. Gold and M. A. Kessick, *J. Chem. Soc.*, 1965, 6718.
²⁸ F. G. Ciapetta and M. Kilpatrick, *J. Amer. Chem. Soc.*, 1948, **70**, 639.
²⁹ (a) A. Ledwith and H. J. Woods, *J. Chem. Soc. (B)*, 1966, 753; (b) A. J. Kresge and W. K. Chang, *J. Amer. Chem. Soc.*, 1978, **100**, 1249.
³⁰ V. M. Cfizmadia, K. M. Koshy, K. C. M. Lau, R. A. McClelland, V. J. Nowlan, and T. T. Tidwell, *J. Amer. Chem. Soc.*, 1979, **101**, 974.
³¹ E. S. Gould, 'Mechanism and Structure in Organic Chemistry,' Holt, Rinehart and Winston, New York, 1959.
³² W. P. Jencks and M. Gilchrist, *J. Amer. Chem. Soc.*, 1964, **86**, 5616.
³³ E. H. Cordes and W. P. Jencks, *J. Amer. Chem. Soc.*, 1962, **84**, 4319.
³⁴ R. B. Martin, A. Parcell, and R. I. Hedrick, *J. Amer. Chem. Soc.*, 1964, **86**, 2406.
³⁵ N. P. Gensmantel and M. I. Page, *J.C.S. Perkin II*, 1979, 137.